

Article

Improvement of Hargreaves–Samani Reference Evapotranspiration Estimates in the Peruvian Altiplano

Apolinario Lujano ^{1,*} , Miguel Sanchez-Delgado ¹  and Efrain Lujano ² ¹ Programa de Maestría en Riego y Drenaje, Universidad Nacional Agraria La Molina, Lima 15024, Peru² Escuela Profesional de Ingeniería Agrícola, Universidad Nacional del Altiplano, Puno 21001, Peru

* Correspondence: 20201311@lamolina.edu.pe

Abstract: The FAO 56 Penman–Monteith equation (PM) is considered the most accurate method for estimating reference evapotranspiration (ET_o). However, PM requires a large amount of data that is not always available. Thus, the objective of this study is to improve the Hargreaves–Samani (HS) reference evapotranspiration estimates in the Peruvian Altiplano (PA) by calibrating the radiation coefficient K_{RS} . The results show modified HS (HSM) ET_o estimates at validation after K_{RS} calibration, revealing evident improvements in accuracy with Nash–Sutcliffe efficiency (NSE) between 0.58 and 0.93, percentage bias (PBIAS) between −0.58 and 1.34%, mean absolute error (MAE) between −0.02 and 0.05 mm/d, and root mean square error (RMSE) between 0.14 and 0.25 mm/d. Consequently, the multiple linear regression (MLR) model was used to regionalize the K_{RS} for the PA. It is concluded that, in the absence of meteorological data, the HSM equation can be used with the new values of K_{RS} instead of HS for the PA.

Keywords: radiation coefficient K_{RS} ; reference evapotranspiration; Hargreaves–Samani; Penman–Monteith



Citation: Lujano, A.; Sanchez-Delgado, M.; Lujano, E. Improvement of Hargreaves–Samani Reference Evapotranspiration Estimates in the Peruvian Altiplano. *Water* **2023**, *15*, 1410. <https://doi.org/10.3390/w15071410>

Academic Editor: Guido D'Urso

Received: 30 January 2023

Revised: 1 March 2023

Accepted: 15 March 2023

Published: 5 April 2023



Copyright: © 2023 by the authors. Licensee MDPI, Basel, Switzerland. This article is an open access article distributed under the terms and conditions of the Creative Commons Attribution (CC BY) license (<https://creativecommons.org/licenses/by/4.0/>).

1. Introduction

Reference evapotranspiration (ET_o) is one of the most useful and necessary indicators for efficient irrigation management [1]. The ET_o plays an important role in estimating the water requirements of crops and irrigation programming, irrigation and drainage design, as well as drought management and studies related to climate change and variation [2–5]. Crop coefficients, which depend on crop characteristics and local conditions, are used to convert ET_o into actual crop evapotranspiration ET_r [6], with accurate estimation of ET_o being of great importance.

In situ measurement of ET_o is expensive and time consuming, and is subject to significant uncertainties. Due to the limitation of in situ measurements of ET_o, several empirical models have been developed for its estimation [7]. The empirical models for ET_o estimation available in the scientific literature are classified as (1) combination models completely based on physics that explain the principles of conservation of mass and energy; (2) semi-physical models that deal with the conservation of mass or energy; and (3) black box models based on artificial neural networks, empirical relationships, and fuzzy and genetic algorithms [8–11].

The method recommended to estimate ET_o by the Food and Agriculture Organization of the United Nations (FAO) is the FAO Penman–Monteith equation 56 (PM) [6,12,13]. ET_o is defined as the evapotranspiration rate of a hypothetical reference crop with an assumed crop height of 0.12 m, a surface resistance of 70 s/m and an albedo of 0.23, very similar to the evapotranspiration of a large area. green grass of uniform height, actively growing, completely shading the ground and not lacking in water [13]. Therefore, the PM equation is written as:

$$ET_{O,PM} = \frac{0.408\Delta(R_n - G) + \gamma 900 U_2 / (T_{mean} + 273)(e_s - e_a)}{\Delta + \gamma(1 + 0.34 U_2)} \quad (1)$$

where $ET_{O,PM}$ is the reference evapotranspiration (mm/d), Δ is the slope of the vapor pressure curve (Kpa/°C), R_n is the net radiation on the crop surface (MJ/m²/d), G is the soil heat flux density (MJ/m²/d), T_{mean} is the mean air temperature (°C), U_2 is the mean wind speed at a height 2 m (m/s), e_s is the saturation vapor pressure (kPa), e_a is the actual vapor pressure (kPa), $e_s - e_a$ is the vapor pressure deficit (kPa) and γ is the psychrometric constant (kPa/°C).

The PM equation was classified as the best to estimate ETo in all types of weather, it can be used globally without any local calibration, since it incorporates physiological and aerodynamic parameters, and has been tested using a variety of lysimeters [1,13]. PM works well in different regions of the world with data on air temperature, relative humidity, solar radiation, and wind speed [14]. However, in places with low availability of meteorological data, its application becomes limited, being the main impediment for the widespread use of the PM equation, therefore, alternative approaches are required to calculate the ETo.

Data limitations motivated Hargreaves and Samani [15] to develop an alternative approach to estimate ETo using only air temperature and extraterrestrial solar radiation data. For this reason, when the necessary meteorological data are not available for the calculation of ETo by the PM method, the Hargreaves–Samani (HS) method is recommended. Due to its simple application for the calculation of ETo with temperature data alone, the focus of research has been the use of the Hargreaves–Samani (HS) equation [15]. This equation can be written as:

$$ET_{O,HS} = 0.0135 \times K_{RS} \times (T_{mean} + 17.8)(T_{max} - T_{min})^{0.5} \times R_a \quad (2)$$

where, $ET_{O,HS}$ corresponds to the reference evapotranspiration of the grass (mm/d), R_a is the extraterrestrial radiation (mm/d), T_{max} , T_{min} y T_{mean} is the maximum, minimum and average temperature (°C), 0.0135 is a conversion factor of units from the American System to the International System, K_{RS} is the adjustment coefficient of the empirical radiation (°C^{-0.5}), and 17.8 is an empirical factor related to the temperature units used in the original formulations.

The empirical K_{RS} coefficient was initially set at 0.17 °C^{-0.5} for arid and semi-arid regions [16]. According to Allen et al. [13], the K_{RS} adjustment coefficient differs for inland or coastal regions, thus, for inland locations where land mass dominates or next to it and where air masses are influenced by a nearby water mass, $K_{RS} = 0.16$ °C^{-0.5}, while for coastal locations with or adjacent to a large land mass where air masses are influenced by a nearby water mass, $K_{RS} = 0.19$ °C^{-0.5}. With R_a in mm/day and the empirical coefficient K_{RS} is normally considered as 0.17 °C^{-0.5}.

Studies carried out under different climatic conditions reported that the calibration of the equations based on air temperature and radiation improved performance [17–19]. In effect, in the scientific literature, various studies worldwide adjusted the coefficients of the original HS equation to improve performance, they also included monthly precipitation [2], for different climatic zones [16], in specific geographic regions regional and local calibration [1,6,17,20–25], others included the altitude of the sites as a variable [26,27], related to the calibration of the radiation coefficient (K_{RS}) [5,28–30]. Therefore, it is very important to investigate the coefficient of radiation (K_{RS}) to reduce the estimation error of the original HS equation, at high altitude and under conditions of the Peruvian Altiplano (PA).

Since the calibration of the K_{RS} of the HS equation can improve the estimates of ETo, we focus this investigation on the main question: Is it possible to improve the reference evapotranspiration estimates of HS in the Peruvian Altiplano? To provide reasonable answers, this article focuses on the principal objective of improving the reference evapotranspiration estimates in the PA through a calibration of the radiation coefficient K_{RS} of the HS equation, under environmental conditions of the PA, and as specific objectives (1) evaluate the original HS equation, (2) calibrate and validate the radiation coefficient K_{RS} of the HS equation, and (3) regionalize the radiation coefficient K_{RS} for the PA based on the geographic characteristics.

2. Materials and Method

2.1. Study Area

The study area is located in the Peruvian Lake Titicaca basin (PLTB). It is characterized as an endorheic basin system surrounded by the eastern and western mountain ranges. It limits to the north with the Amazon hydrographic region, to the south-west with the Pacific hydrographic region and to the east with the PLT of the Republic of Bolivia, with an altitude (Figure 1a) that varies from 3804 to 5781 m.a.s.l. According to the climatic classification of Peru, the PLT has a predominantly rainy climate type, with dry autumn and winter [31].

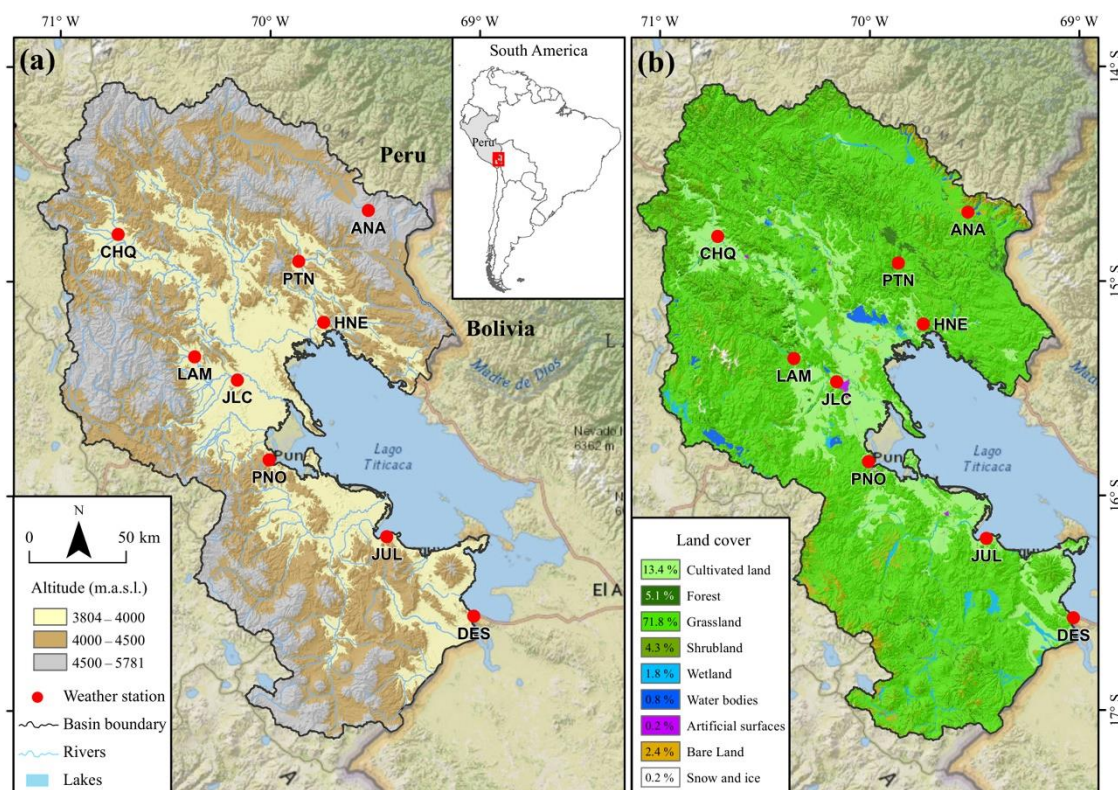


Figure 1. (a) Location of the study area and spatial distribution of weather stations and (b) land cover.

The study area has an average annual rainfall that varies from 624.9 mm to 948.3 mm. The maximum and minimum air temperatures for all seasons range between 10.5 and 17.8 °C, and −2.2 and 3.5 °C, respectively. The relative humidity varies between 55% and 80.6%, while the wind speed oscillates between 1.5 and 5.5 m/s. The sun hours are between 6.3 and 8.4 h, and the altitudes of the stations are between 3812 and 4660 m.a.s.l. On the other hand, the aridity index (AI) for the meteorological station sites varies between 0.54 and 0.78 (mean 0.64). The AI is defined as the relationship between the annual precipitation (P) and the annual reference evapotranspiration (ET₀) [32]. Then, the weather station sites are climatically classified as dry sub-humid (SH-s) to humid sub-humid (SH-h) (Table 1) according to the AI levels defined for Peru by Huerta and Lavado [32].

According to GlobeLand30 version 2010, the dominant land cover type for the PA is grassland, followed by cultivated land, forest, shrubland, bare land, wetland, water bodies, snow and ice, and artificial surfaces. GlobeLand30 is a 30 m spatial resolution global land cover data product developed by China [33], with versions available for 2000, 2010 and 2020 (<http://www.globallandcover.com>: accessed on 16 February 2023). Most weather stations are located on grassland (PTN, JLC and PNO), cultivated land (CHQ, HNE and JUL) and Artificial surfaces (ANA and DES) (Figure 1b).

Table 1. Coordinates of the weather stations used, average of the meteorological variables, aridity index and climatic classification.

Station	Lat.	Long.	Alt.	T _{max}	T _{min}	Rh	U ₂	Sh	ETo	P	AI	CC
Ananea (ANA)	−14.676	−69.534	4660	10.5	−1.9	80.6	2.0	6.3	2.7	658.4	0.67	SH-h
Lampa (LAM)	−15.361	−70.374	3866	17.1	−0.3	55.0	2.4	8.1	3.6	757.1	0.60	SH-d
Chuquibambilla (CHQ)	−14.788	−70.728	3918	16.3	−2.2	61.3	2.1	7.2	3.2	787.0	0.67	SH-h
Putina (PTN)	−14.921	−69.876	3861	17.3	0.1	70.1	2.6	6.9	3.1	643.9	0.56	SH-d
Huancané (HNE)	−15.207	−69.758	3840	15.7	0.3	58.9	2.9	7.7	3.4	650.5	0.52	SH-d
Juliaca (JLC)	−15.444	−70.208	3838	17.8	−0.5	75.0	1.5	7.8	3.2	624.9	0.53	SH-d
Puno (PNO)	−15.826	−70.012	3812	16.3	3.5	61.1	1.8	8.1	3.5	750.6	0.59	SH-d
Juli (JUL)	−16.204	−69.460	3830	14.1	3.0	58.3	2.4	8.4	3.5	948.3	0.78	SH-h
Desaguadero (DES)	−16.563	−69.037	3833	15.2	1.7	65.7	5.5	7.4	3.4	736.9	0.60	SH-d

2.2. Climatic and Terrain Data

The data used for this study are monthly values of maximum (T_{max}, °C) and minimum (T_{min}, °C) air temperature, relative humidity (RH, %), sun hours (SH, h), wind speed (U₁₀, m/s) at a height of 10 m and precipitation (P, mm) from nine weather stations distributed in the PA (Figure 1a). The selected stations have data records from 2000 to 2019 (information provided by the National Meteorology and Hydrology Service of Peru (SENAMHI)). The stations considered include the representative stations of the PA, defined on the basis of the aridity index suggested by Huerta and Lavado [32].

A quality control process of the rain gauge measurements was carried out, which consisted of the verification of specific physical limits for the Peruvian territory, internal consistency, and spatial consistency [34]. The homogeneity of the climatic variables Rh, U₁₀, Sh, T_{max}, T_{min} and P were analyzed by means of a visual inspection, and the absolute method. For the absolute method, the nonparametric test of Distribution-free cumulative sum (CUSUM) and rank-sum (RS) were applied independently to the data from each weather station using the TREND program (<https://toolkit.ewater.org.au/Tools/TREND>: accessed on 10 August 2022). CUSUM, is a nonparametric test of step jump in the mean, while RS is a nonparametric test of difference in the mean of two periods [35]. The null hypothesis for CUSUM and RS suggests that there is no step jump in the mean in the data series, and there is no difference in the mean between two data periods, which accepts the null hypothesis if the maximum deviation for CUSUM and the statistic z for calculated RS are less than the critical value of the statistical table at the 5% significance level and rejects it otherwise. Thus, the doubtful periods of the Rh, U₁₀, Sh, T_{max}, T_{min} and P data series that did not meet the assumption of homogeneity were not considered in subsequent analyses.

In effect, the missing values were filled in using the random forest (RF) machine learning algorithm incorporated in the MICE (Generates Multivariate Imputations by Chained Equations) package for the R project [36]. It should be noted that the homogeneity of the data was checked with monthly data after filling in the missing data [37,38]. Homogeneity tests are generally more robust when used with monthly data [37]. The wind speed at a height of 2 m (U₂, m/s) was calculated from U₁₀.

Lat south latitude; Long west longitude; Alt altitude (m.a.s.l.); Rh relative humidity (%); U₂ wind speed (m/s) at a height of 2 m; Sh sun hours (h); ETo reference evapotranspiration estimated by the PM method (mm/d); P annual precipitation (mm/year); AI aridity index; CC climatic classification; SH-h subhumid-humid; SH-d subhumid-dry.

To regionalize the K_{RS} radiation coefficient calibrated from the HS equation, the NASA Shuttle Radar Topography Mission (SRTM) digital elevation model (DEM) was obtained from the Google Earth Engine (GEE) platform available at <https://earthengine.google.com/> (accessed on 15 July 2022), ID de la imagen CGIAR/SRTM90_V4 [39], with a spatial resolution of ~90 m.

Figure 2 shows that the climatic and geographical variables that affect the ETo. As the altitude increases, precipitation, reference evapotranspiration, minimum and maximum

temperature, sun hours and wind speed decrease, on the contrary, relative humidity increases, for the weather stations under study.

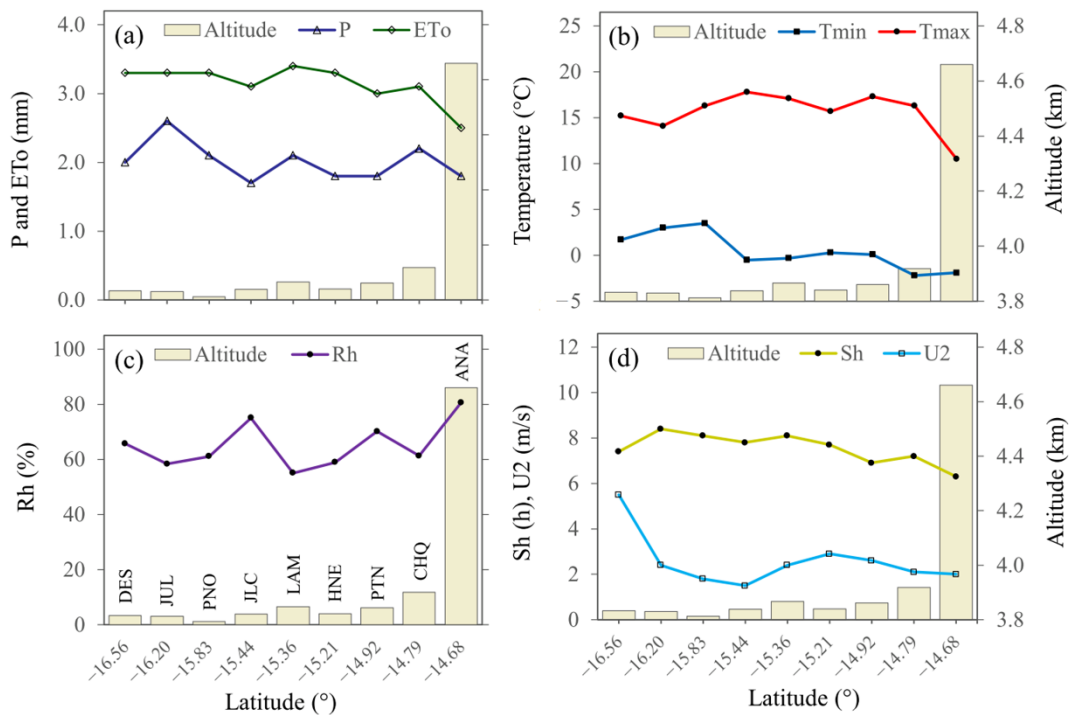


Figure 2. Variation of climatic factors as a function of latitude and altitude (a) P and ETo (b) T_{min} and T_{max}, (c) Rh and (d) Sh and U₂.

2.3. Evaluation of the Original Hargreaves-Samani Equation for Use in the Peruvian Altiplano

In this study, the PM method has been used as a substitute for reference evapotranspiration measured data, being the standard procedure when no lysimeter measured data is available [20]. Due to the lack of experimental reference evapotranspiration (ETo) measurements, the numbers given by the PM equation have been accepted as the true values. Moreover, this equation has been used to calibrate the modified versions of the Hargreaves-Samani (HS) equations [13,16].

The calculation of all the data required for the estimation of the ETo followed the recommendations given in the manual 56 of Irrigation and Drainage of the FAO [6].

$$R_s = \left(a_s + b_s \frac{n}{N} \right) R_a \tag{3}$$

where R_a is the extraterrestrial radiation ($\text{MJ}/\text{m}^2/\text{d}$), n is the actual duration of sunlight (h), N is the maximum possible duration of sunlight or hours of sunlight (h), a_s is the regression constant which expresses the fraction of extraterrestrial radiation that reaches the earth on cloudy days ($n = 0$) and $a_s + b_s$ is the fraction of extraterrestrial radiation that reaches the earth on clear days ($n = N$). In the absence of real measurements and calibration of solar radiation (R_s), values suggested by Allen et al. [13] are $a_s = 0.25$ and $b_s = 0.50$. However, these default values should not be applied to high altitude sites, where proper calibration is required [40]. In this regard, values of $a_s = 0.23$ and $b_s = 0.60$ suggested by Chipana et al. [3], were used for high altitude areas (3820 to 3950 m.a.s.l.) estimated for the Bolivian altiplano and for altitudes above the 4660 m.a.s.l. was considered with slight modifications of $a_s = 0.29$ and $b_s = 0.55$.

Extraterrestrial radiation (R_a) was estimated using the equation recommended by Allen et al. [13]. The values of R_a for each day of the year and for different latitudes can be estimated from the solar constant, the solar declination and the time of the year and then

selecting the R_a for the 15th day of each month converted to monthly values, using the following equation:

$$R_a = \frac{24(60)}{\pi} G_{SC} d_r [\omega_s \sin(\varnothing) \sin(\delta) + \cos(\varnothing) \cos(\delta) \sin(\omega_s)] \quad (4)$$

where G_{SC} is the solar constant = 0.0820 MJ/m²/min, d_r is the inverse relative distance to the sun, ω_s is the hour angle of sunset (rad), \varnothing is the latitude (rad), and δ is the solar declination (rad).

The net radiation (R_n) was calculated as the difference between the incoming net shortwave radiation (R_{ns}) and the outgoing net longwave radiation (R_{nl}).

$$R_n = R_{ns} - R_{nl} \quad (5)$$

To calculate the net incoming shortwave radiation (R_{ns}), the value used for albedo was 0.23, while the net longwave radiation (R_{nl}), was estimated using the expression postulated by the modified Stefan-Boltzmann law due to absorption and downward radiation from the sky [13].

$$R_{nl} = \sigma \left[\frac{T_{max,K}^4 + T_{min,K}^4}{2} \right] (0.34 - 0.14\sqrt{e_a}) \times \left(1.35 \frac{R_s}{R_{s0}} - 0.35 \right) \quad (6)$$

where R_{nl} is the net longwave radiation (MJ/m²/d), σ is the Stefan-Boltzmann constant (4.903×10^{-9} MJ/K⁻⁴/m²/d), $T_{max,K}^4$ is the maximum absolute temperature during the 24 h period ($K = ^\circ C + 273$), $T_{min,K}^4$ is the minimum absolute temperature during the 24 h period ($K = ^\circ C + 273$), e_a is the actual vapor pressure (kPa), R_s/R_{s0} is the relative shortwave radiation (limited a ≤ 1.0), R_s is the calculated solar radiation (MJ/m²/d) and R_{s0} is the calculated clear-sky radiation (MJ/m²/d).

The vapor pressure deficit is calculated as the difference between the saturation vapor pressure (e_s) and the actual vapor pressure (e_a). e_s is calculated as the average of the saturation vapor pressure at T_{max} and T_{min} . Approximations can be used to estimate e_a depending on the available data. When only daily mean relative humidity (RH_{mean}) data is available, e_a is calculated as [13]:

$$e_a = \frac{RH_{mean}}{100} \left[\frac{e^o(T_{max}) + e^o(T_{min})}{2} \right] \quad (7)$$

2.4. Statistical Performance Metrics

To evaluate the performance between the original HS and the PM method for the nine weather stations, statistical performance metrics were used (Table 2), including the correlation coefficient (R), the Nash–Sutcliffe efficiency coefficient (NSE) used by Almorox and Grieser [16] and Todorovic et al. [4], percent bias (PBIAS), and root mean square error (RMSE) and mean absolute error (MAE), both used by Cobaner et al. [25].

The R denotes the degree of correlation between the observed and calculated values of ETo, with values ranging from -1.0 to 1.0 , where values closer to ± 1 indicate a better association between them. Legates and McCabe [41] suggest using the NSE coefficient to assess goodness of fit. [42] defined the coefficient of efficiency ranging from minus infinity to 1.0 , where higher values indicate a better relationship. The NSE indicates that when the residual variance is equal to the variance of the observed data, the result is $NSE = 1.0$. On the contrary, when the NSE is equal to zero or is negative, it indicates that the observed mean is as good or a better predictor than the model. [43] classified the performance of a model as very good if $NSE > 0.75$, good if $0.65 < NSE \leq 0.75$, satisfactory if $0.50 < NSE \leq 0.65$ and poor if $NSE \leq 0.50$.

Table 2. List of statistical performance metrics used for the calibration and validation of the K_{RS} of the HS equation for the estimation of ETo.

Statistical Performance	Equation ¹	Unit	Optimal Value
Correlation coefficient (R)	$R = \frac{\sum_{i=1}^N (ET_{O,PM} - \overline{ET}_{O,PM})(ET_{O,HS} - \overline{ET}_{O,HS})}{\sqrt{\sum_{i=1}^N (ET_{O,PM} - \overline{ET}_{O,PM})^2} \sqrt{\sum_{i=1}^N (ET_{O,HS} - \overline{ET}_{O,HS})^2}}$	-	±1
Nash–Sutcliffe efficiency (NSE)	$ENS = 1.0 - \frac{\sum_{i=1}^N (ET_{O,PM} - ET_{O,HS})^2}{\sum_{i=1}^N (ET_{O,PM} - \overline{ET}_{O,PM})^2}$	-	1
Percent bias (PBIAS)	$PBIAS = \frac{\sum_{i=1}^N (ET_{O,HS} - ET_{O,PM})}{\sum_{i=1}^N ET_{O,PM}} \times 100$	%	0
Mean absolute error (MAE)	$MAE = \frac{1}{N} \sum_{i=1}^N ET_{O,HS} - ET_{O,PM} $	mm	0
Root mean square error (RMSE)	$RMSE = \sqrt{\frac{1}{N} \sum_{i=1}^N (ET_{O,HS} - ET_{O,PM})^2}$	mm	0

Notes: ¹ Variables: $ET_{O,PM}$ is the estimated value with PM, $ET_{O,HS}$ is the calculated value, $\overline{ET}_{O,PM}$ is the average of the estimated value with PM, $\overline{ET}_{O,HS}$ is the average of the calculated value, and N is the total number of data.

Instead, PBIAS indicates the average trend of simulated data based on larger or smaller observed data, with the best value being 0 and negative (positive) values indicating an underestimation (overestimation) [44]. According to the criteria of Moriasi et al. [45], the statistical performance of models can be considered ‘very good’ when $PBIAS < \pm 5$, ‘good’ when $\pm 5 \leq PBIAS < \pm 10$, ‘satisfactory’ when $\pm 10 \leq PBIAS < \pm 25$ and ‘not satisfactory’ when $PBIAS \geq \pm 25$.

On the other hand, [46] indicate that the MAE is the most natural measure of the magnitude of the average error of the absolute differences between what is observed and calculated. A low MAE value implies a high performance of the model. Meanwhile, the RMSE is one of the commonly used error rates [16], and it follows that a smaller RMSE indicates a better approximation of the model.

2.5. Calibration and Validation of the Radiation Coefficient K_{RS} of the HS Equation

Todorovic et al. [4] reported that it is preferable to adjust the values of K_{RS} than to change the coefficient of 0.0023. Under this perspective, the HS equation was modified by means of calibrating the K_{RS} expressed as:

$$ET_{O,HSM} = 0.0135 \times \hat{K}_{RS} \times R_a \times (T_{med} + 17.8)(T_{max} - T_{min})^{0.5} \tag{8}$$

The \hat{K}_{RS} of the HS equation was adjusted using the ETo data determined by the PM method, \hat{K}_{RS} and was calibrated using the generalized reduced gradient (GRG) non-linear resolution method of the Microsoft Excel Solver tool. To define the objective function, the maximization of the ENS function (Nash–Sutcliffe coefficient of efficiency) and the minimization of the RMSE function (root mean square error) were established as the optimization objective in the Solver tool.

Shiri et al. [47] report that testing the calibrated version using the same calibration data could lead to partially valid results. Therefore, the observed data corresponding to the period from 2000 to 2019 were separated into two groups, being considered for calibration (70%) and validation (30%). However, using historical data to calibrate the HS model directly ignores the continuity of climate change over time, which can lead to good performance of the calibrated HS model in the calibrated years; however, instability may appear when the HS model is an extended data set [48]. To reduce this instability, the calibration and validation period was selected randomly. Consequently, to verify the validity of the new \hat{K}_{RS} obtained from the HS equation, they were evaluated through performance metrics, which that include the ENS, PBIAS, MAE and RMSE (Table 2).

2.6. Regionalization of the Radiation Coefficient \hat{K}_{RS}

A geographic information system (GIS) was used to spatially interpolate the point values of \hat{K}_{RS} at a spatial resolution of ~90 m. The multiple linear regression (MLR) method was used with \hat{K}_{RS} as the dependent variable, while the longitude, latitude and altitude

were used as independent variables followed by residual values. The longitude and latitude maps were interpolated using the inverse distance weighted (IDW) method based on the pixel centroids of the altitude map, while the residue map was interpolated using the IDW method based on point location values of each weather station. Next, \hat{K}_{RS} was obtained using map algebra (raster calculator tool) in ArcGIS. The value of $\hat{K}_{RS(x)}$ at the unmeasured points is obtained according to the following equation:

$$\hat{K}_{RS(x)} = b_0 + b_1 \times X + b_2 \times Y + b_3 \times Z + residue \tag{9}$$

where: $\hat{K}_{RS(x)}$ is the predicted value at point x , b_0 , b_1 , b_2 and b_3 are the MRL coefficients, the values of X , Y and Z are the independent variables at point x , X is the longitude, Y is the latitude, Z is the altitude, and the residue.

The flow diagram of Figure 3 summarizes the analysis procedure for the improvement of the Hargreaves–Samani reference evapotranspiration estimates.

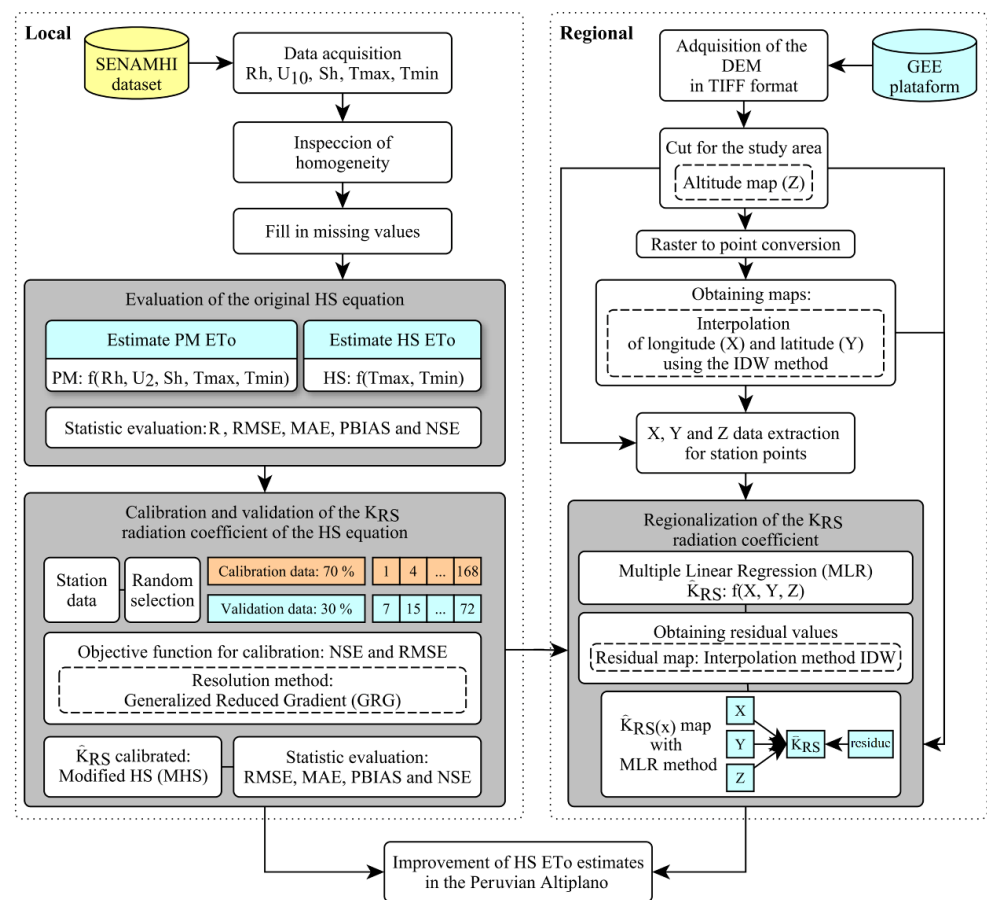


Figure 3. Flow diagram for the improvement of the Hargreaves–Samani reference evapotranspiration estimates in the PA.

3. Results and Discussion

3.1. Evaluation of the Original Hargreaves–Samani Equation

Figure 4 illustrates the comparison of ETo estimates by the original HS method versus the PM method. The value of K_{RS} considered for the HS equation was $0.17 \text{ } ^\circ\text{C}^{-0.5}$ for all weather stations. The precision of the ETo values of the original HS equation had significant variations in the SH-h and SH-d climatic zones identified in the study area (Table 1). The scatter diagrams reveal that the values of the correlation coefficient (R) within the two climatic zones oscillated between 0.84 and 0.97, presenting lower values in the ANA and PTN stations and higher values in the PNO and JLC stations. On the other hand, in relation to the values of the NSE vary between -0.57 and 0.87 , NSE values lower than

0.50 were presented in the PTN, JUL, JLC and ANA stations, indicating poor performance. Meanwhile, values higher than 0.75 were presented in the of HNE and LAM stations, indicating very good performance according to the discretion of Moriasi et al. [43].

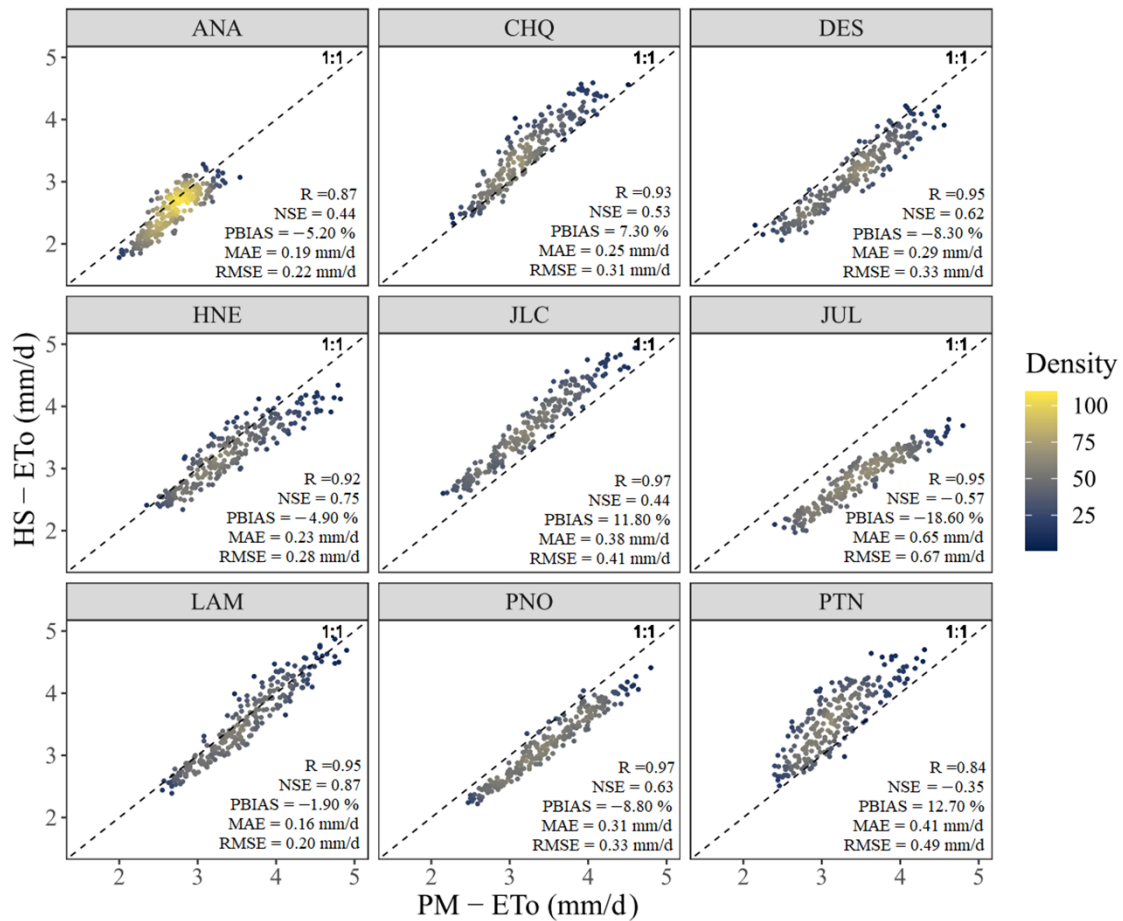


Figure 4. Scatter diagrams between values of ETo by the PM method versus original HS at the weather stations.

The PBIAS oscillates values between -18.60% and 12.70% , deducing that the HS equation tends to underestimate the ETo in the JUL, PNO, DES, ANA. HNE and LAM stations with values of -18.60% , -8.80% , -8.30% , -5.20% , -4.90% and -1.90% , respectively. On the other hand, it tends to overestimate the ETo in the PTN, JLC and CHQ stations with values of 12.70% , 11.80% , and 7.30% respectively. The ETo underestimations occurred in the JUL, PNO, DES y HNE stations that are close to Lake Titicaca (LT), it was also observed in the LAM and ANA stations that are far from the LT, while the overestimations the ETo observed in the stations that are far from the LT. For the CHQ station that is in the SH-h climate classification, and the JLC and PTN stations with SH-d climate, the results are in accordance with that determined by Trajkovic [6], where the HS model generally overestimates the ETo in humid climate areas. However, the ANA and JUL station with the SH-h climate and DES, HNE, LAM and PNO stations with the SH-d climate, underestimated the ETo, therefore, the use of the HS equation is not very efficient.

Meanwhile, for Allen et al. [13], the HS equation tends to underestimate the ETo values under strong wind conditions and to overestimate the ETo under high relative humidity conditions. In this study, only the DES station reports a high wind speed, which tends to underestimate the ETo, while the other stations that registered lower wind speeds tended to underestimate and overestimate the ETo. On the other hand, in relation to relative humidity, the results do not agree with the ANA weather station, which tends to underestimate ETo.

On the other hand, the values of the MAE oscillate between 0.16 and 0.65 mm/d, presenting the lowest values in the LAM, ANA, HNE, CHQ and DES stations (0.16, 0.19, 0.23, 0.25 and 0.29 mm/d) and the high values in the PNO, JLC, PTN and JUL stations (0.31, 0.38, 0.41 and 0.65 mm/d). Likewise, the RMSE values vary between 0.20 and 0.67 mm/d, presenting low values occurred in the LAM, ANA, HNE, CHQ, DES and PUN stations (0.20, 0.22, 0.28, 0.31, 0.33 and 0.33 mm/d) and high values in the JLC, PTN and JUL stations (0.41, 0.49 and 0.67 mm/d).

3.2. Calibration and Validation of the Radiation Coefficient K_{RS} of the HS Equation

The results show that using a single value of K_{RS} can lead to less precise estimates of ETo in the PA, thus, the calibrated values of the \hat{K}_{RS} range from $0.150\text{ }^{\circ}\text{C}^{-0.5}$ to $0.199\text{ }^{\circ}\text{C}^{-0.5}$. For most of the stations, the values of \hat{K}_{RS} differ from the coefficient suggested by Hargreaves and Samani [15], except that of the LAM station where a very close value was obtained ($\hat{K}_{RS} = 0.173\text{ }^{\circ}\text{C}^{-0.5}$). High values of \hat{K}_{RS} were obtained at the DES, JUL, PNO and HNE stations close to LT, with values of $0.184\text{ }^{\circ}\text{C}^{-0.5}$, $0.209\text{ }^{\circ}\text{C}^{-0.5}$, $0.186\text{ }^{\circ}\text{C}^{-0.5}$ and $0.179\text{ }^{\circ}\text{C}^{-0.5}$, respectively, while low \hat{K}_{RS} values were obtained at the CHQ, JLC and PTN stations with values of $0.158\text{ }^{\circ}\text{C}^{-0.5}$, $0.152\text{ }^{\circ}\text{C}^{-0.5}$ and $0.150\text{ }^{\circ}\text{C}^{-0.5}$ respectively, which are the same ones that are far from the LT. The ANA station located at high altitude (4660 m.a.s.l.) and far from the LT registered a high value of $\hat{K}_{RS} = 0.179\text{ }^{\circ}\text{C}^{-0.5}$. Ref. [30] showed that K_{RS} values do not decrease with distance from the sea. At the same time, the standard values of $0.16\text{ }^{\circ}\text{C}^{-0.5}$ and $0.19\text{ }^{\circ}\text{C}^{-0.5}$ should not be assumed. In this regard, the precision of the ETo estimate improved for each weather station by adopting the calibrated and validated \hat{K}_{RS} values in the HS equation.

Figure 5 shows the spatial distribution of the NSE, PBIAS, MAE and RMSE of the ETo estimates from the HS and modified HS equation (HSM) for the nine stations. The performance indicators significantly improved the NSE values that oscillate between 0.64 and 0.94 for the calibration phase, while for the validation phase the NSE values oscillate between 0.58 to 0.93. The lowest values were presented in the ANA and PTN stations with 0.64 and 0.65 in the calibration phase, and values of 0.58 and 0.64 in the validation phase.

On the other hand, the PBIAS values oscillate between -0.52% and -0.01% in the calibration phase, presenting slight underestimations in all weather stations; however, in the validation phase the values oscillate between -0.58% and 1.34% , presenting underestimations in the CHQ and DES stations at -0.21% and -0.58% respectively, according to the discretion of Moriasi et al. [43] the PBIAS values are below $\pm 5\%$, being considered 'very good'.

Regarding the MAE, the HSM equation with calibrated and validated \hat{K}_{RS} values presents low values for all weather stations, ranging between 0.02 and 0.00 mm/d, for the calibration phase. Meanwhile, for the validation phase, the MAE values oscillate between -0.02 and 0.05 mm/d, respectively. Likewise, for the calibration phase, the RMSE values are between 0.13 and 0.25 mm/d, while for the validation phase, the RSME values are between 0.14 and 0.25 mm/d. The precision indicators used agree with those found in studies conducted by Rodrigues and Braga [30], Paredes et al. [29] and Raziei and Pereira [5], where, after calibrating the value of the K_{RS} , the ETo led to very good results, being able to use the simplified equations (Table 3) for the estimation of the ETo locally.

3.3. Regionalisation of the Radiation Coefficient \hat{K}_{RS}

Considering the scarcity of climatic data, the regionalization of the \hat{K}_{RS} for the PA is proposed. The RLM model was used to build the regionalization model of the \hat{K}_{RS} based on geographic characteristics. The results of the correlation analysis between \hat{K}_{RS} and the geographical characteristics of longitude, latitude and altitude resulted in a correlation equal to 0.59, -0.62 and 0.04 respectively. The latitude feature obtained the highest correlation compared with the longitude and altitude features. Consequently, the geographical characteristics (longitude, latitude and altitude) explained the variability of \hat{K}_{RS} by 55.7% ($R^2 = 0.557$) (Figure 6b). This study found that the regional equation of $\hat{K}_{RS(x)}$ could better

estimate ETo for regions with limited data within the PA, with the magnitude of R^2 being acceptable for estimating \hat{K}_{RS} in the PA from geographic characteristics.

$$\hat{K}_{RS(x)} = -0.271560 + 0.000879 \times X - 0.024670 \times Y + 0.000032 \times Z + residue \quad (10)$$

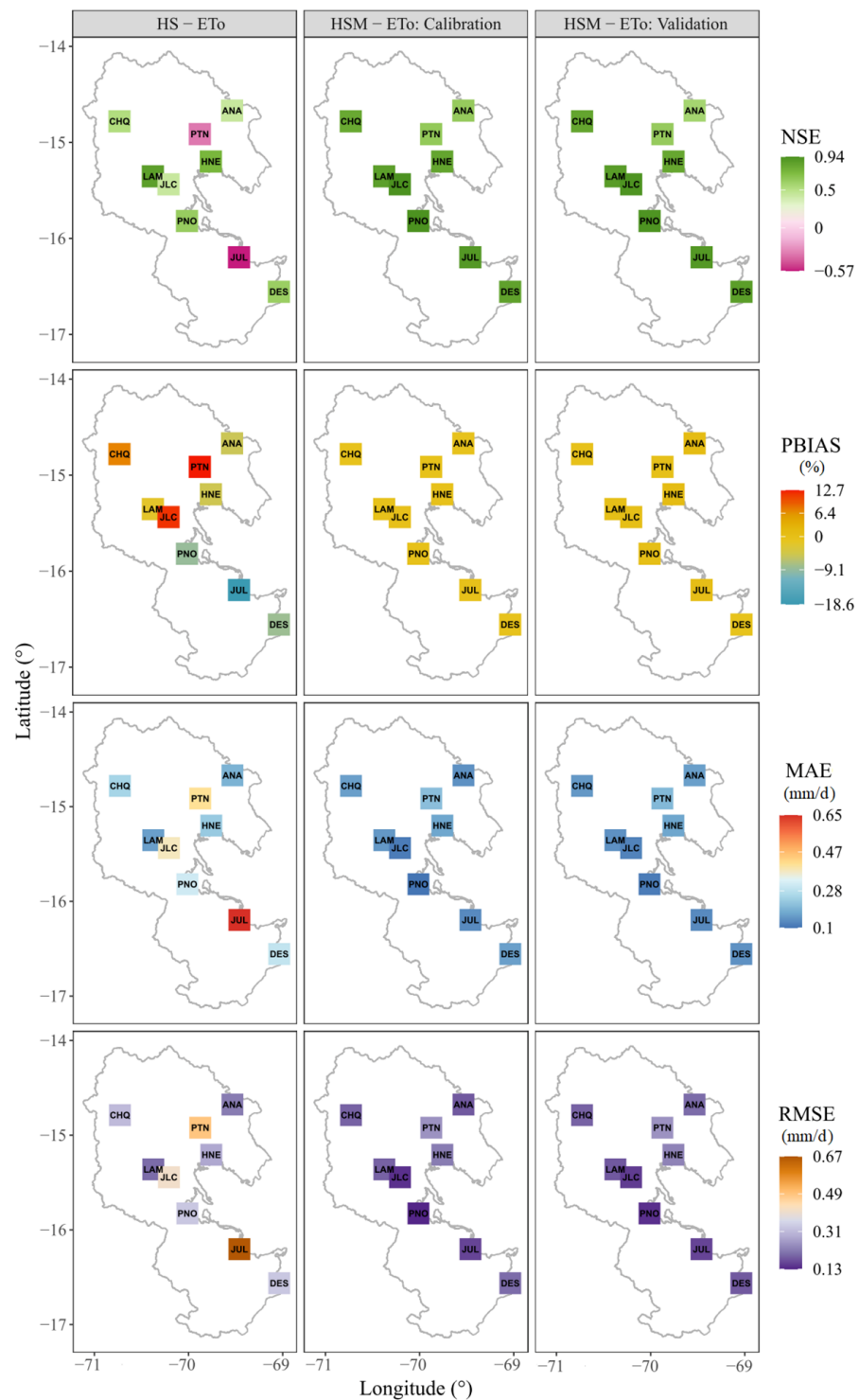


Figure 5. Spatial distribution of the NSE, PBIAS (%), MAE (mm/d) and RMSE (mm/d) from the ETo estimates of HS with original K_{RS} , HSM with \hat{K}_{RS} in the calibration and validation phase. Study area in gray outline.

Table 3. Modified HS equations for each weather station.

Station	Recommended Equations
Ananea (ANA)	$ET_{O,HSM(ANA)} = 0.0135 \times 0.179 \times R_a \times (T_{med} + 17.8)(T_{max} - T_{min})^{0.5}$
Lampa (LAM)	$ET_{O,HSM(LAM)} = 0.0135 \times 0.173 \times R_a \times (T_{med} + 17.8)(T_{max} - T_{min})^{0.5}$
Chuquibambilla (CHQ)	$ET_{O,HSM(CHQ)} = 0.0135 \times 0.158 \times R_a \times (T_{med} + 17.8)(T_{max} - T_{min})^{0.5}$
Putina (PTN)	$ET_{O,HSM(PTN)} = 0.0135 \times 0.150 \times R_a \times (T_{med} + 17.8)(T_{max} - T_{min})^{0.5}$
Huancané (HNE)	$ET_{O,HSM(HNE)} = 0.0135 \times 0.179 \times R_a \times (T_{med} + 17.8)(T_{max} - T_{min})^{0.5}$
Juliaca (JLC)	$ET_{O,HSM(JLC)} = 0.0135 \times 0.152 \times R_a \times (T_{med} + 17.8)(T_{max} - T_{min})^{0.5}$
Puno (PNO)	$ET_{O,HSM(PNO)} = 0.0135 \times 0.186 \times R_a \times (T_{med} + 17.8)(T_{max} - T_{min})^{0.5}$
Juli (JUL)	$ET_{O,HSM(JUL)} = 0.0135 \times 0.209 \times R_a \times (T_{med} + 17.8)(T_{max} - T_{min})^{0.5}$
Desaguadero (DES)	$ET_{O,HSM(DES)} = 0.0135 \times 0.184 \times R_a \times (T_{med} + 17.8)(T_{max} - T_{min})^{0.5}$

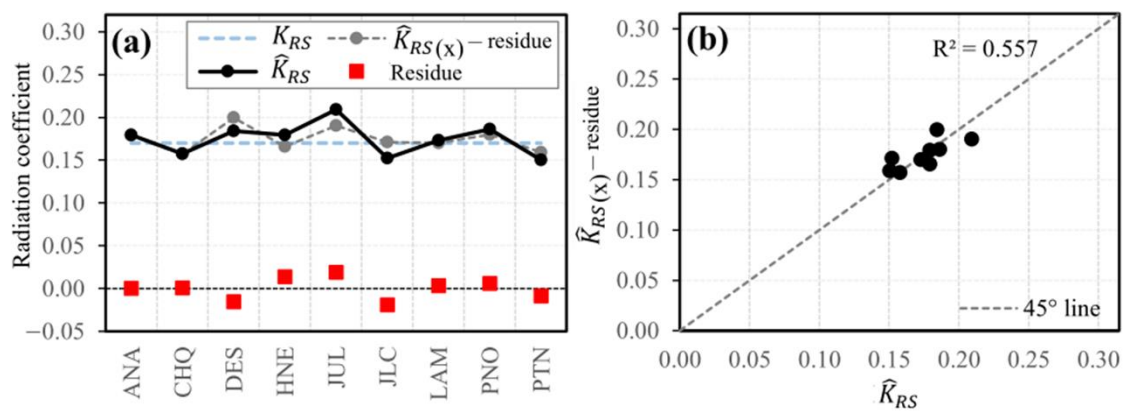


Figure 6. Regionalization of the calibrated radiation coefficient \hat{K}_{RS} of the HS equation as a function of longitude, latitude and altitude: (a) variation of the original K_{RS} , \hat{K}_{RS} calibrated, $\hat{K}_{RS(x)} - residue$ and residuals; (b) scatterplot between \hat{K}_{RS} and $\hat{K}_{RS(x)} - residue$ interpolated without addition of the residual.

The standard error for \hat{K}_{RS} was 0.016. The confidence interval for the b_0 model parameter varies between -4.25303 and 3.70991 , that for b_1 varies between -0.04514 and 0.04690 , that for b_2 varies between -0.06647 and 0.01713 and that for b_3 varies between -0.00005 and 0.00012 , with a confidence level of 95%. The residuals of \hat{K}_{RS} for the station points, vary between -0.019 and 0.019 respectively (Figure 6a), being the applicable equation for the PA.

The $\hat{K}_{RS(x)}$ values for the PA vary between 0.15 and 0.27. The spatial distribution is greater for the western, central and southern zone of the Altiplano, as it approaches the coastal areas; while lower values are observed for the northern zone there (Figure 7), these estimated values when regionalizing the radiation coefficient for the PA, are found in the range of the values reported by Samani [49] which oscillates between 0.12 and $0.24 \text{ } ^\circ\text{C}^{-0.5}$, by Raziei and Pereira [5] obtained values that oscillate between 0.14 and $0.20 \text{ } ^\circ\text{C}^{-0.5}$, while results obtained by Paredes et al. [50] show values that oscillate between 0.14 and $0.25 \text{ } ^\circ\text{C}^{-0.5}$, respectively.

The regional equation to estimate the ETo in the PA based on the Hargreaves–Samani model is as follows:

$$ET_{O,HSM} = 0.0135 \times \hat{K}_{RS(x)} \times R_a \times (T_{med} + 17.8)(T_{max} - T_{min})^{0.5} \tag{11}$$

where $\hat{K}_{RS(x)}$, is the predicted value at any point in the Peruvian Altiplano.

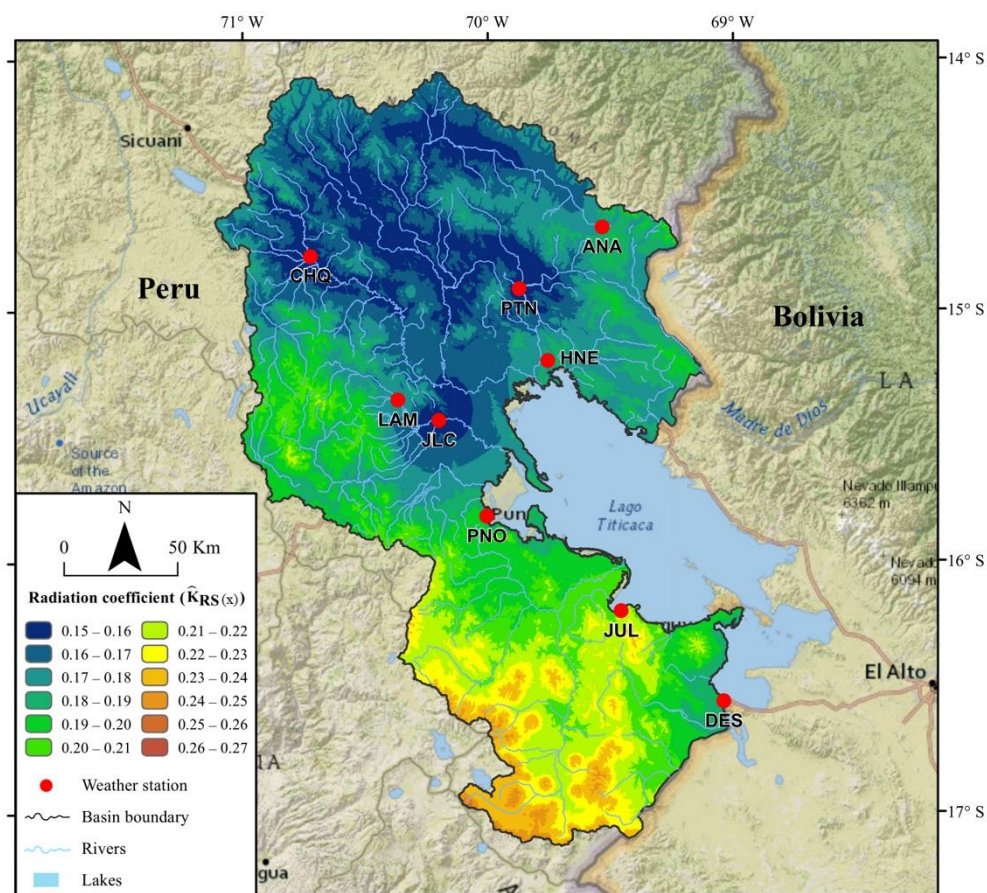


Figure 7. Spatial distribution of the radiation coefficient $\hat{K}_{RS}(x)$.

4. Conclusions

The main objective of the research was to improve the Hargreaves–Samani reference evapotranspiration estimates in the PA. The main conclusions are summarized below:

The HS model based on air temperature is recommended as the simplest and most practical method to estimate ETo. The ETo HS estimates were evaluated based on the ETo PM estimates in the PA. The period considered was from January 2000 to December 2019 on a monthly time scale. The ETo calculated with PM and HS showed a high correlation, but a great bias, with strong underestimations and overestimations of the ETo, requiring its local calibration before its use.

Due to its association of the radiation coefficient K_{RS} with solar radiation, it is preferable to calibrate the values of K_{RS} from the HS equation and thus obtain an HSM equation. The HSM model performed better than the HS model for each weather station. Better estimates of ETo were obtained with HSM after calibration of the radiation coefficient K_{RS} of the HS equation, mainly removing biases.

The new values of the radiation coefficient K_{RS} of the HS empirical model for the PA are presented. The MLR model was used to regionalize the radiation coefficient K_{RS} . The HS equation, together with the calibrated radiation coefficient K_{RS} , can significantly improve the estimate of ETo over data-deficient regions within the PA.

It is important to note that although the MLR model used to regionalize the KRS has proven effective in estimating ETo in the study area, it is necessary to consider that the lack of availability of observed climatic data could affect its reliability in areas far from the meteorological stations used for calibration. Therefore, caution is recommended when using the HS equation with new KRS values in areas outside the study area and away from the meteorological stations, and further research is suggested to evaluate the applicability of the proposed approach in other regions with different climatic and topographic conditions.

In this regard, future research lines could be explored, such as (1) examining the influence of other factors, such as soil moisture and vegetation cover, on the accuracy of ETo estimates using the HS model, (2) expanding the research to other regions with different climatic and topographic conditions to evaluate the applicability of the proposed methodology, and (3) exploring the regionalization of KRS based on additional climatic factors. These research lines could improve the accuracy of ETo estimates and, therefore, have a positive impact on the management and planning of water resources in different regions.

Author Contributions: Conceptualization, A.L., M.S.-D. and E.L.; methodology, A.L. and E.L.; formal analysis, E.L.; investigation, A.L. and E.L.; resources, A.L., M.S.-D. and E.L.; writing—original draft preparation, A.L. and E.L.; writing review and editing, A.L., M.S.-D. and E.L. All authors have read and agreed to the published version of the manuscript.

Funding: This research received no external funding.

Data Availability Statement: Not applicable.

Acknowledgments: Our thanks to the National Service of Meteorology and Hydrology (SENAMHI)—Peru for providing the meteorological information for carrying out this research study.

Conflicts of Interest: The authors declare no conflict of interest.

References

- Berti, A.; Tardivo, G.; Chiaudani, A.; Rech, F.; Borin, M. Assessing reference evapotranspiration by the Hargreaves method in north-eastern Italy. *Agric. Water Manag.* **2014**, *140*, 20–25. [[CrossRef](#)]
- Droogers, P.; Allen, R.G. Estimating reference evapotranspiration under inaccurate data conditions. *Irrig. Drain. Syst.* **2002**, *16*, 33–45. [[CrossRef](#)]
- Chipana, R.; Yujra, R.; Paredes, P.; Pereira, L.S. Determinación de la evapotranspiración de referencia con datos limitados en zonas de altura del Altiplano Boliviano aplicando la metodología de la FAO y la ecuación de Hargreaves-Samani. In *I Congreso Boliviano de Riego y Drenaje*; Facultad de Agronomía: La Paz, Argentina, 2010; pp. 12–14.
- Todorovic, M.; Karic, B.; Pereira, L.S. Reference Evapotranspiration estimate with limited weather data across a range of Mediterranean climates. *J. Hydrol.* **2013**, *481*, 166–176. [[CrossRef](#)]
- Raziei, T.; Pereira, L.S. Estimation of ETo with Hargreaves–Samani and FAO-PM temperature methods for a wide range of climates in Iran. *Agric. Water Manag.* **2013**, *121*, 1–18. [[CrossRef](#)]
- Trajkovic, S. Hargreaves versus Penman-Monteith under Humid Conditions. *J. Irrig. Drain. Eng.* **2007**, *133*, 38–42. [[CrossRef](#)]
- Muhammad, M.K.I.; Nashwan, M.S.; Shahid, S.; Ismail, T.B.; Song, Y.H.; Chung, E.S. Evaluation of empirical reference evapotranspiration models using compromise programming: A case study of Peninsular Malaysia. *Sustainability* **2019**, *11*, 4267. [[CrossRef](#)]
- Adamala, S.; Raghuwanshi, N.S.; Mishra, A.; Tiwari, M.K. Evapotranspiration modeling using second-order neural networks. *J. Hydrol. Eng.* **2014**, *19*, 1131–1140. [[CrossRef](#)]
- Srivastava, A.; Sahoo, B.; Raghuwanshi, N.S.; Singh, R. Evaluation of Variable-Infiltration Capacity Model and MODIS-Terra Satellite-Derived Grid-Scale Evapotranspiration Estimates in a River Basin with Tropical Monsoon-Type Climatology. *J. Irrig. Drain. Eng.* **2017**, *143*, 4017028. [[CrossRef](#)]
- Kumari, N.; Srivastava, A. An Approach for Estimation of Evapotranspiration by Standardizing Parsimonious Method. *Agric. Res.* **2020**, *9*, 301–309. [[CrossRef](#)]
- Hamed, M.M.; Khan, N.; Muhammad, M.K.I.; Shahid, S. Ranking of Empirical Evapotranspiration Models in Different Climate Zones of Pakistan. *Land* **2022**, *11*, 2168. [[CrossRef](#)]
- Pereira, L.S.; Allen, R.G.; Smith, M.; Raes, D. Crop evapotranspiration estimation with FAO56: Past and future. *Agric. Water Manag.* **2015**, *147*, 4–20. [[CrossRef](#)]
- Allen, R.G.; Pereira, L.S.; Raes, D.; Smith, M. Crop evapotranspiration: Guidelines for computing crop water requirements. FAO Irrigation and drainage paper 56. *FAO Rome* **1998**, *300*, D05109.
- Almorox, J.; Senatore, A.; Quej, V.H.; Mendicino, G. Worldwide assessment of the Penman–Monteith temperature approach for the estimation of monthly reference evapotranspiration. *Theor. Appl. Climatol.* **2018**, *131*, 693–703. [[CrossRef](#)]
- Hargreaves, G.H.; Samani, Z.A. Reference Crop Evapotranspiration from Temperature. *Appl. Eng. Agric.* **1985**, *1*, 96–99. [[CrossRef](#)]
- Almorox, J.; Grieser, J. Calibration of the Hargreaves–Samani method for the calculation of reference evapotranspiration in different Köppen climate classes. *Hydrol. Res.* **2016**, *47*, 521–531. [[CrossRef](#)]
- Bogawski, P.; Bednorz, E. Comparison and validation of selected evapotranspiration models for conditions in Poland (Central Europe). *Water Resour. Manag.* **2014**, *28*, 5021–5038. [[CrossRef](#)]
- Čadro, S.; Uzunović, M.; Žurovec, J.; Žurovec, O. Validation and calibration of various reference evapotranspiration alternative methods under the climate conditions of Bosnia and Herzegovina. *Int. Soil Water Conserv. Res.* **2017**, *5*, 309–324. [[CrossRef](#)]

19. Awal, R.; Habibi, H.; Fares, A.; Deb, S. Estimating reference crop evapotranspiration under limited climate data in West Texas. *J. Hydrol. Reg. Stud.* **2020**, *28*, 100677. [[CrossRef](#)]
20. Gavilán, P.; Lorite, I.J.; Tornero, S.; Berengena, J. Regional calibration of Hargreaves equation for estimating reference et in a semiarid environment. *Agric. Water Manag.* **2006**, *81*, 257–281. [[CrossRef](#)]
21. Tabari, H.; Talaee, P.H. Local calibration of the Hargreaves and Priestley-Taylor equations for estimating reference evapotranspiration in arid and cold climates of Iran based on the Penman-Monteith model. *J. Hydrol. Eng.* **2011**, *16*, 837. [[CrossRef](#)]
22. Mohawesh, O.E.; Talazi, S.A. Comparison of Hargreaves and FAO56 equations for estimating monthly evapotranspiration for semi-arid and arid environments. *Arch. Agron. Soil Sci.* **2012**, *58*, 321–334. [[CrossRef](#)]
23. Pandey, V.; Pandey, P.K.; Mahanta, A.P. Calibration and performance verification of Hargreaves Samani equation in a humid region. *Irrig. Drain.* **2014**, *63*, 659–667. [[CrossRef](#)]
24. Dorji, U.; Olesen, J.E.; Seidenkrantz, M.S. Water balance in the complex mountainous terrain of Bhutan and linkages to land use. *J. Hydrol. Reg. Stud.* **2016**, *7*, 55–68. [[CrossRef](#)]
25. Cobaner, M.; Citakoğlu, H.; Haktanir, T.; Kisi, O. Modifying Hargreaves–Samani equation with meteorological variables for estimation of reference evapotranspiration in Turkey. *Hydrol. Res.* **2017**, *48*, 480–497. [[CrossRef](#)]
26. Ravazzani, G.; Corbari, C.; Morella, S.; Gianoli, P.; Mancini, M. Modified Hargreaves–Samani equation for the assessment of reference evapotranspiration in Alpine river basins. *J. Irrig. Drain. Eng.* **2012**, *138*, 592–599. [[CrossRef](#)]
27. Lavado Casimiro, W.S.; Lhomme, J.P.; Labat, D.; Guyot, J.L.; Boulet, G. Estimación de la evapotranspiración de referencia (FAO-56 Penman-Monteith) con limitados datos climáticos en la cuenca andina amazónica peruana. *Rev. Peru. Geo Atmosférica* **2015**, *4*, 31–43.
28. Morales-Salinas, L.; Ortega-Farías, S.; Riveros-Burgos, C.; Neira-Román, J.; Carrasco-Benavides, M.; López-Olivari, R. Monthly calibration of Hargreaves–Samani equation using remote sensing and topoclimatology in central-southern Chile. *Int. J. Remote Sens.* **2017**, *38*, 7497–7513. [[CrossRef](#)]
29. Paredes, P.; Fontes, J.C.; Azevedo, E.B.; Pereira, L.S. Daily reference crop evapotranspiration in the humid environments of Azores islands using reduced data sets: Accuracy of FAO-PM temperature and Hargreaves–Samani methods. *Theor. Appl. Climatol.* **2018**, *134*, 595–611. [[CrossRef](#)]
30. Rodrigues, G.C.; Braga, R.P. Estimation of Reference Evapotranspiration during the Irrigation Season Using Nine Temperature-Based Methods in a Hot-Summer Mediterranean Climate. *Agriculture* **2021**, *11*, 124. [[CrossRef](#)]
31. Servicio Nacional de Meteorología e Hidrología del Perú (SENAMHI). *Climas del Perú—Mapa de Clasificación Climática Nacional*; Dirección de Meteorología y Evaluación Ambiental Atmosférica: Lima, Perú, 2020.
32. Huerta, A.; Lavado, W. *ATLAS Zonas Áridas Del Perú: Una Evaluación Presente Y Futura*; SENAMHI: Lima, Perú, 2021.
33. Chen, J.; Chen, J.; Liao, A.; Cao, X.; Chen, L.; Chen, X.; He, C.; Han, G.; Peng, S.; Lu, M.; et al. Global land cover mapping at 30 m resolution: A POK-based operational approach. *ISPRS J. Photogramm. Remote Sens.* **2015**, *103*, 7–27. [[CrossRef](#)]
34. Vera, L.; Villegas, E.; Oria, C.; Arboleda, F. *Control de Calidad de Datos de Estaciones Meteorológicas E Hidrológicas Automáticas en El Centro de Procesamiento de Datos Del SENAMHI*; Servicio Nacional de Meteorología e Hidrología del Perú (SENAMHI): Lima, Perú, 2021.
35. Chiew, F.H.; Siriwardena, L. *Trend/Change Detection Software. USER GUIDE*; CRC for Catchment Hydrology: Clayton, Australia, 2005.
36. Van Buuren, S.; Groothuis-Oudshoorn, K. Mice: Multivariate imputation by chained equations in R. *J. Stat. Softw.* **2011**, *45*, 1–67. [[CrossRef](#)]
37. Tomas-Burguera, M.; Vicente-Serrano, S.M.; Beguería, S.; Reig, F.; Latorre, B. Reference 634 crop evapotranspiration database in Spain (1961–2014). *Earth Syst. Sci. Data.* **2019**, *11*, 1917–1930. [[CrossRef](#)]
38. Woldeesenbet, T.A.; Elagib, N.A.; Ribbe, L.; Heinrich, J. Gap filling and homogenization of climatological datasets in the headwater region of the Upper Blue Nile Basin, Ethiopia. *Int. J. Climatol.* **2017**, *37*, 2122–2140. [[CrossRef](#)]
39. Jarvis, A.; Reuter, H.I.; Nelson, A.; Guevara, E. Hole-Filled SRTM for the Globe Version 4. Available from the CGIAR-CSI SRTM 90m Database. 2008. Available online: <http://srtm.csi.cgiar.org> (accessed on 15 July 2022).
40. Ye, J.; Guo, A.; Sun, G. Statistical analysis of reference evapotranspiration on the Tibetan Plateau. *J. Irrig. Drain. Eng.* **2009**, *135*, 134–140. [[CrossRef](#)]
41. Legates, D.R.; McCabe, G.J. Evaluating the use of ‘goodness-of-fit’ measures in hydrologic and hydroclimatic model validation. *Water Resour. Res.* **1999**, *35*, 233–241. [[CrossRef](#)]
42. Nash, J.E.; Sutcliffe, J.V. River flow forecasting through conceptual models part I—A discussion of principles. *J. Hydrol.* **1970**, *10*, 282–290. [[CrossRef](#)]
43. Moriasi, D.; Arnold, J.; Van Liew, M.; Bingner, R.; Harmel, R.; Veith, T. Model evaluation guidelines for systematic quantification of accuracy in watershed simulations. *Trans. ASABE* **2007**, *50*, 885–900. [[CrossRef](#)]
44. Vu, T.T.; Li, L.; Jun, K.S. Evaluation of multi-satellite precipitation products for streamflow simulations: A case study for the Han River Basin in the Korean Peninsula, East Asia. *Water* **2018**, *10*, 642. [[CrossRef](#)]
45. Moriasi, D.N.; Gitau, M.W.; Pai, N.; Daggupati, P. Hydrologic and water quality models: Performance measures and evaluation criteria. *Trans. ASABE* **2015**, *58*, 1763–1785.
46. Willmott, C.J.; Matsuura, K. Advantages of the mean absolute error (MAE) over the root mean square error (RMSE) in assessing average model performance. *Clim. Res.* **2005**, *30*, 79–82. [[CrossRef](#)]

47. Shiri, J.; Sadraddini, A.A.; Nazemi, A.H.; Marti, P.; Fard, A.F.; Kisi, O.; Landeras, G. Independent testing for assessing the calibration of the Hargreaves–Samani equation: New heuristic alternatives for Iran. *Comput. Electron. Agric.* **2015**, *117*, 70–80. [[CrossRef](#)]
48. Feng, Y.; Jia, Y.; Cui, N.; Zhao, L.; Li, C.; Gong, D. Calibration of Hargreaves model for reference evapotranspiration estimation in Sichuan basin of southwest China. *Agric. Water Manag.* **2017**, *181*, 1–9. [[CrossRef](#)]
49. Samani, Z. Discussion of “History and Evaluation of Hargreaves Evapotranspiration Equation” by George H. Hargreaves and Richard G. Allen. *J. Irrig. Drain. Eng.* **2003**, *130*, 447. [[CrossRef](#)]
50. Paredes, P.; Fontes, J.C.; Azevedo, E.B.; Pereira, L.S. Daily reference crop evapotranspiration with reduced data sets in the humid environments of Azores islands using estimates of actual vapor pressure, solar radiation, and wind speed. *Theor. Appl. Climatol.* **2018**, *134*, 1115–1133. [[CrossRef](#)]

Disclaimer/Publisher’s Note: The statements, opinions and data contained in all publications are solely those of the individual author(s) and contributor(s) and not of MDPI and/or the editor(s). MDPI and/or the editor(s) disclaim responsibility for any injury to people or property resulting from any ideas, methods, instructions or products referred to in the content.